Memoirs of the Faculty of Engineering, Nagoya University
Vol. 36, No. 1 (1984) — Research Report —

THE NUMERICAL ANALYSIS OF TRANSONIC FLOW AROUND A CIRCULAR AIRFOIL USING HYBRID DIFFERENCE SCHEME

YI-YUN WANG and TOSHI FUJIWARA

Department of Aeronautical Engineering
Nagoya University, Nagoya 464, Japan

Abstract

A mixed difference scheme called hybrid scheme, which is initiated in Reference 1 and is shown to be effective particularly for computation of transonic flow, is applied to calculate the transonic flow around a circular airfoil. The result is compared with those obtained by the MacCormack scheme and the hybrid one in Reference 1.

1. Introduction

In parallel with the appearance of super computers, the numerical experiment has become one of the most important techniques solving problems of aerodynamics. In comparison with general wind tunnel experiments, it possesses the advantages of shorter testing time and less cost. Corresponding to the development of computers, numerical methods also achieved rapid growth in the last decade. The finite difference method is regarded as the most powerful and versatile among all the existing methods. Besides its simplicity of algorithm, it can be transformed into parallel operations more easily than the others.

The appearance of the MacCormack scheme is an important development for the finite difference method. It is a two-step, second-order-accurate and non-centered scheme and has been used most widely nowadays. Its advantages are well-known, but it usually causes spurious oscillations in numerical solutions ahead of shock and is subjected to an excessively rigorous stability restriction. Warming and Beam [1] introduced a new scheme called the upwind scheme, which can reduce the spurious oscillations and has twice as wide stability bounds as the M-scheme; but it can only be used in the region where the characteristic speeds have the same sign. Based on the above-mentioned development, they suggested to use a combination of the M and U-schemes, called the hybrid scheme, for the computa-

tion of a transonic flow: The M-scheme is used where the flow is subsonic while the U-scheme is used where the flow is supersonic.

In Reference 1, a series of theoretical problems related to the H-scheme are stated in detail. We followed their analysis of a transonic flow around a circular airfoil with the 10% thickness-to-chord ratio and the freestream Mach number of 0.83, almost identically using their techniques. The obtained results favorably restate some of the conclusions in Reference 1. Naturally the accuracy must be improved in the future calculation.

2. The Difference Scheme in One-Dimensional System

For the numerical solution of a hyperbolic system in a conservation form

$$\frac{\partial U}{\partial t}+\frac{\partial F(U)}{\partial x}=0, \tag{1}$$

where $U=(u_1, u_2, \cdots, u_m)$, the M-scheme is written as

$$\overline{U_i^{n+1}}=U_i^n-\frac{\Delta t}{\Delta x}\nabla F_i^n, \tag{2}$$

$$U_i^{n+1}=\frac{1}{2}(U_i^n+\overline{U_i^{n+1}})-\frac{\Delta t}{2\Delta x}\Delta\overline{F_i^{n+1}}, \tag{3}$$

where U_i^n denotes the finite-difference approximation of $U(n\Delta t, i\Delta x)$, while the forward and backward difference operators are defined by

$$\Delta F_i=F_{i+1}-F_i, \quad \nabla F_i=F_i-F_{i-1}. \tag{4}$$

The operators (2) and (3) are called predictor and corrector, respectively. The M-scheme is a two-step explicit scheme with second-order accuracy in both time and space.

There is not a stringent verification for the stability of nonlinear equations up to now. One always linearizes them locally, then uses classical methods for linearized equations. Thus, if λ_l $(l=1, 2, \cdots, m)$ are the local eigenvalues of the Jacobian matrix $\partial F/\partial U$ (all of them are real since the system (1) is hyperbolic), using the standard von Neumann method, the amplification factor $G_l(k)$ for the M-scheme is

$$G_l(k)=1-\nu_l^2(1-\cos k\Delta x)-i\cdot\nu_l\sin k\Delta x, \tag{5}$$

and

$$|G_l(k)|^2=1-\nu_l^2(1-\nu_l)^2(1-\cos k\Delta x)^2. \tag{6}$$

Hence, the necessary and sufficient condition for stability of the M-scheme results in

$$|\nu_l|=|\lambda_l|\Delta t/\Delta x\leqslant 1, \tag{7}$$

i. e.,

$$\Delta t/\Delta x \leqslant \mathrm{Min}\{1/|\lambda_1|,\ 1/|\lambda_2|,\ \cdots,\ 1/|\lambda_m|\}. \tag{8}$$

It should be noted that $|G_l(k)|$ can not attenuate when the corresponding local eigenvalue λ_l is equal to zero. In order to increase the dissipation, a simple way is to append to the right-hand side of the M-scheme (3) the fourth-order dissipative term

$$-\frac{\omega}{8}\delta^4 U_i^n = -\frac{\omega}{8}(Q_i^n - Q_{i-1}^n), \tag{9}$$

where

$$Q_h = U_{h+2} - 3U_{h+1} + 3U_h - U_{h-1} \qquad (h=i,\ i-1). \tag{10}$$

The parameter ω is a positive number limited by the condition that all the $|G_l(k)|$ are not to exceed 1:

$$G_l(k) = 1 - \nu_l^2(1-\cos k\Delta x) - i\cdot\nu_l \sin k\Delta x - \omega(1-\cos k\Delta x)^2/2, \tag{11}$$

and therefore,

$$|G_l(k)|^2 = [1-\nu_l^2(1-\cos k\Delta x) - \omega(1-\cos k\Delta x)^2/2]^2 + \nu_l^2 \sin^2 k\Delta x. \tag{12}$$

The $|G_l(k)|^2$ becomes maximum or minimum when $\sin k\Delta x = 0$, i. e.,

$$|G_l(k)|^2 = 1 \qquad \text{when } k\Delta x = 0,$$

$$|G_l(k)|^2 = (1-2\nu_l^2-2\omega)^2 \qquad \text{when } k\Delta x = \pi.$$

If $(1-2\nu_l^2-2\omega)^2 < 1$, then obviously 1 is the maximum, $(1-2\nu_l^2-2\omega)^2$ is the minimum and the scheme is still stable. Therefore,

$$0 \leqslant \omega < 1-\nu_l^2 \qquad (l=1,\ 2,\ \cdots,\ m), \tag{13}$$

or

$$0 \leqslant \omega < \mathrm{Min}\{1-\nu_1^2,\ 1-\nu_2^2,\ \cdots,\ 1-\nu_m^2\}. \tag{14}$$

The U-scheme possesses the predictor (2) identical to the M-scheme, while the corrector is constructed as follows:

$$U_i^{n+1} = \frac{1}{2}(U_i^n + \overline{U_i^{n+1}}) - \frac{\Delta t}{2\Delta x}\nabla \overline{F_i^{n+1}} - \frac{\Delta t}{2\Delta x}\nabla^2 F_i^n. \tag{15}$$

It is an explicit two-step scheme having second-order accuracy in both time and space as well. The amplification factor of the U-scheme is

$$G_l(k) = 1 - \nu_l[\nu_l + (1-\nu_l)(1-\cos k\Delta x)](1-\cos k\Delta x)$$
$$- i\cdot\nu_l \sin k\Delta x \cdot [1 + (1-\nu_l)(1-\cos k\Delta x)], \tag{16}$$

and accordingly,

$$|G_l(k)|^2 = 1 - \nu_l(1-\nu_l)^2(2-\nu_l)(1-\cos k\Delta x)^2. \tag{17}$$

Hence, the stability condition for the U-scheme is

$$0 \leqslant \nu_l = \lambda_l \Delta t / \Delta x \leqslant 2. \tag{18}$$

From the left-hand side of the inequality (18), it is demanded that all the eigenvalues must be of the same sign; in other words, they are all positive here (if they are all negative, the U-scheme can be altered by replacing ∇ by Δ, and ∇^2 by $-\Delta^2$ in Eqs. (2) and (15)). From the right-hand side of the inequality (18), it is clear that the U-scheme has twice the stability bound of the M-scheme.

The U-scheme is not used when an eigenvalue is equal to zero; therefore the fourth-order dissipative term is not necessary.

The problems in transforming between the M and U-schemes arise when they are mixedly used to calculate the same flow field. The M-U and U-M transition operators have to suffice the conservation laws. Thus, the M-U transition operator consists of only the predictor (2) with no corrector; the one-step process. In fact, it is the first-order upwind scheme that is first-order accurate. Its stability bound is contained in that of the U-scheme. The U-M transition operator is

$$U_i^{n+1} = U_i^n - \frac{\Delta t}{2\Delta x}(\overline{F_{i+1}^{n+1}} - \overline{F_{i-1}^{n+1}}) - \frac{\Delta t}{2\Delta x}\nabla^2 F_i^n, \tag{19}$$

which is first-order accurate as well and can be proved unstable. It is difficult to analyze the stability even for smooth solutions of a scalar conservation law when an unstable scheme such as Eq. (19) is used at only one point. Numerical experiments show that the stability is not overturned when placing the U-M transition point at appropriate location.

Summarizing the above four difference approximations, they can be rewritten in the following:

$$\begin{aligned} U_i^{n+1} = {} & \frac{1}{2}(U_i^n + \overline{U_i^{n+1}}) - \frac{\Delta t}{2\Delta x}[\varepsilon_i F_i^n - (\varepsilon_i + \varepsilon_{i-1})F_{i-1}^n + \varepsilon_{i-1}F_{i-2}^n] \\ & - \frac{\Delta t}{2\Delta x}[-\varepsilon_{i-1}\overline{F_{i-1}^{n+1}} + (\varepsilon_i + \varepsilon_{i-1} - 1)\overline{F_i^{n+1}} + (1-\varepsilon_i)\overline{F_{i+1}^{n+1}}] \\ & - \frac{\omega}{8}[(1-\varepsilon_i)Q_i^n - (1-\varepsilon_{i-1})Q_{i-1}^n], \end{aligned} \tag{20}$$

where $\overline{U_i^{n+1}}$, Q_i^n and Q_{i-1}^n are determined by Eqs, (2) and (10), and

$$(\varepsilon_{i-1}, \varepsilon_i) = \begin{cases} (0, 0) & \text{M-scheme,} \\ (0, 1) & \text{M-U transition operator,} \\ (1, 1) & \text{U-scheme,} \\ (1, 0) & \text{U-M transition operator.} \end{cases} \tag{21}$$

3. Time Splitting Technique for Two-Dimensional System

Consider a two-dimensional system in the conservation form

$$\frac{\partial U}{\partial t}+\frac{\partial F}{\partial x}+\frac{\partial G}{\partial y}=0, \tag{22}$$

to which the following time splitting technique can be applied:

$$U_{i,j}^{n+1}=L_X(\Delta t)L_Y(\Delta t)U_{i,j}^{n}. \tag{23}$$

This means that the solution of Eq. (22) is obtained as a result of multiplying the two operators sequentially; $L_Y(\Delta t)$ solving the equation

$$\frac{\partial U}{\partial t}+\frac{\partial G}{\partial y}=0, \tag{24}$$

and $L_X(\Delta t)$ solving the equation

$$\frac{\partial U}{\partial t}+\frac{\partial F}{\partial x}=0. \tag{25}$$

However, the solution (23) is only first-order accurate. Second-order accuracy can be retained at every other time step by reversing the sequence of operators;

$$U_{i,j}^{n+2}=L_Y(\Delta t)L_X(\Delta t)L_X(\Delta t)L_Y(\Delta t)U_{i,j}^{n}. \tag{26}$$

Therefore, second-order accuracy can be maintained at every time step by defining

$$U_{i,j}^{n+1}=L_Y(\Delta t/2)L_X(\Delta t)L_Y(\Delta t/2)U_{i,j}^{n}. \tag{27}$$

This conclusion still holds when x and y are interchanged.

Using the time splitting technique not only simplifies the calculation of every step but also has less strict stability criteria. It is analogical with the conclusion for the following simple example. The stability criterion of the equation

$$\frac{\partial \zeta}{\partial t}+u\frac{\partial \zeta}{\partial x}=0 \qquad (u\geqslant 0) \tag{28}$$

is

$$u\frac{\Delta t}{\Delta x}\leqslant 1, \tag{29}$$

whereas that of the equation

$$\frac{\partial \zeta}{\partial t}+u\frac{\partial \zeta}{\partial x}+v\frac{\partial \zeta}{\partial y}=0 \qquad (u\geqslant 0,\ v\geqslant 0) \tag{30}$$

is

$$u\frac{\Delta t}{\Delta x}+v\frac{\Delta t}{\Delta y}\leqslant 1. \tag{31}$$

Obviously, the condition (31) is more strict than (29).

The stability conditions for Eq. (27) are

$$\frac{(\Delta t/2)}{\Delta y} \leqslant \mathrm{Min}\{1/|\mu_1|,\ 1/|\mu_2|,\ \cdots,\ 1/|\mu_m|\}, \tag{32}$$

and

$$\frac{\Delta t}{\Delta x} \leqslant \mathrm{Min}\{1/|\lambda_1|,\ 1/|\lambda_2|,\ \cdots,\ 1/|\lambda_m|\} \qquad \text{(M-scheme)} \tag{33}$$

or

$$\frac{\Delta t}{\Delta x} \leqslant \mathrm{Min}\{2/\lambda_1,\ 2/\lambda_2,\ \cdots,\ 2/\lambda_m\} \qquad \text{(U-scheme)} \tag{34}$$

where λ_l and μ_l are the eigenvalues of $\partial F/\partial U$ and $\partial G/\partial U$, respectively.

4. Calculation of Example

Applying the foregoing theory, we calculated the steady inviscid flow field around a circular airfoil with the thickness-to-chord ratio $\delta/L=0.1$. The free-stream is uniform and parallel with the chord of the airfoil (Fig. 1). The free-stream Mach number is high enough to produce an embedded supersonic region over a portion of airfoil surface.

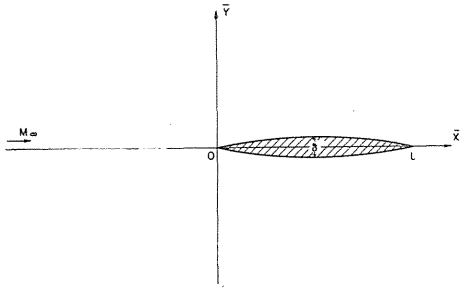

Fig. 1. Transonic flow around a circular airfoil with thickness-to-chord ratio $\delta/L=0.1$.

The gasdynamic equations are

$$\frac{\partial U}{\partial t}+\frac{\partial F}{\partial x}+\frac{\partial G}{\partial y}=0, \tag{35}$$

$$U=\begin{pmatrix}\rho\\ \rho u\\ \rho v\\ e\end{pmatrix}, \qquad F=\begin{pmatrix}\rho u\\ \rho u^2+p\\ \rho uv\\ (e+p)u\end{pmatrix}, \qquad G=\begin{pmatrix}\rho v\\ \rho uv\\ \rho v^2+p\\ (e+p)v\end{pmatrix}, \tag{36}$$

$$p=(\gamma-1)\left[e-\frac{1}{2}\rho(u^2+v^2)\right] \qquad (\gamma=1.40). \tag{37}$$

The variables ρ, u, v, p and e in Eq. (36) are the dimensionless density $\bar{\rho}/\bar{\rho}_\infty$, X-direction velocity component $\bar{u}/\bar{u}_\infty$, Y-direction velocity component $\bar{v}/\bar{u}_\infty$, pressure $\bar{p}/\bar{\rho}_\infty\bar{u}_\infty^2$ and total energy per unit volume $\bar{e}/\bar{\rho}_\infty\bar{u}_\infty^2$, respectively. The variables t, x and y in Eq. (35) are the dimensionless time $\bar{t}\,\bar{u}_\infty/L$, coordinates $\bar{x}/L$ and $\bar{y}/L$, respectively.

The grid generation is shown in Fig. 2. Calculated points are the central locations of meshes, along with the points on airfoil surface and symmetric axis [2]. Regarding the meshes over the circular airfoil surface, the M-scheme $L_{MY}(\Delta t)$ (Y-direction) is

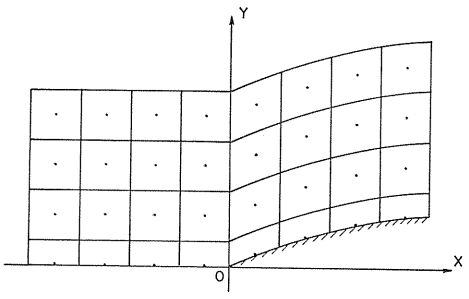

Fig. 2. Mesh points and cell system.

$$U_{i,j}^{n+1/2}=U_{i,j}^{n}-\frac{\Delta t}{\Delta y}\nabla H_{i,j}^{n}, \tag{38}$$

$$U_{i,j}^{n+1/2}=\frac{1}{2}(U_{i,j}^{n}+U_{i,j}^{\overline{n+1/2}})-\frac{\Delta t}{2\Delta y}\Delta H_{i,j}^{\overline{n+1/2}}, \tag{39}$$

$$H_{i,j}=\frac{\Delta s_i}{\Delta x}(\cos\bar{\theta}_i\cdot G_{i,j}-\sin\bar{\theta}_i\cdot F_{i,j}), \tag{40}$$

where $\tan\bar{\theta}_i$ is the average inclination of the i-th circular arc and Δs_i is its length. Since the eigenvalues of $\partial(\cos\bar{\theta}\cdot G-\sin\bar{\theta}\cdot F)/\partial U$ are $(\cos\bar{\theta}\cdot v-\sin\bar{\theta}\cdot u)$, $(\cos\bar{\theta}\cdot v-\sin\bar{\theta}\cdot u)$, $(\cos\bar{\theta}\cdot v-\sin\bar{\theta}\cdot u)+c$ and $(\cos\bar{\theta}\cdot v-\sin\bar{\theta}\cdot u)-c$ (c=local sonic velocity), they have mixed signs when $|v|$ is rather small, rendering us to use the M-scheme. In connection with X-direction, the eigenvalues of $\partial F/\partial U$ are u, u, $u+c$ and $u-c$, having mixed signs in nearly subsonic regions ($u\leqslant c$) and all positive in nearly supersonic regions ($u>c$). It is possible to use the H-scheme $L_{HX}(\Delta t)$, that is,

$$U_{i,j}^{\overline{n+1/2}}=U_{i,j}^{n}-\frac{\Delta t}{\Delta x}\nabla F_{i,j}^{n}, \tag{41}$$

$$\begin{aligned}U_{i,j}^{n+1/2}=&\frac{1}{2}(U_{i,j}^{n}+U_{i,j}^{\overline{n+1/2}})-\frac{\Delta t}{2\Delta x}[\varepsilon_i F_{i,j}^{n}-(\varepsilon_i+\varepsilon_{i-1})F_{i-1,j}^{n}+\varepsilon_{i-1}F_{i-2,j}^{n}]\\&-\frac{\Delta t}{2\Delta x}[-\varepsilon_{i-1}F_{i-1,j}^{\overline{n+1/2}}+(\varepsilon_i+\varepsilon_{i-1}-1)F_{i,j}^{\overline{n+1/2}}+(1-\varepsilon_i)F_{i+1,j}^{\overline{n+1/2}}]\\&-\frac{\omega}{8}[(1-\varepsilon_i)Q_{i,j}^{n}-(1-\varepsilon_{i-1})Q_{i-1,j}^{n}],\end{aligned} \tag{42}$$

$$(\varepsilon_{i-1},\ \varepsilon_i)=\begin{cases}(0,\ 0) & u_{i,j}^{\overline{n+1/2}}\leqslant c_{i,j}^{\overline{n+1/2}},\\ (0,\ 1) & u_{i,j}^{\overline{n+1/2}}>c_{i,j}^{\overline{n+1/2}}\ \text{and}\ u_{i-1,j}^{n+1/2}\leqslant c_{i-1,j}^{n+1/2},\\ (1,\ 1) & u_{i,j}^{\overline{n+1/2}}>c_{i,j}^{\overline{n+1/2}},\ u_{i-1,j}^{n+1/2}>c_{i-1,j}^{n+1/2}\ \text{and}\ u_{i+1,j}^{n}>c_{i+1,j}^{n},\\ (1,\ 0) & u_{i,j}^{\overline{n+1/2}}>c_{i,j}^{\overline{n+1/2}}\ \text{and}\ u_{i+1,j}^{n}\leqslant c_{i+1,j}^{n}.\end{cases}\quad\text{when} \tag{43}$$

It should be noted that the U-M transition point must be placed at the last supersonic point ahead of shock. It implies that the variables at that point should be determined not only by the upstream supersonic points but also by the adjacent downstream subsonic point. If the shock conditions can not be satisfied there, then it is possible to move the shock wave forward or backward.

Replacing the eigenvalues μ_l and λ_l of Eqs. (32), (33) and (34) by the practical eigenvalues of this example, the stability conditions are

$$L_{MY}(\Delta t/2):\ \frac{(\Delta t/2)}{\Delta y}\leqslant \mathrm{Min}\left\{\frac{(\Delta x/\Delta s_i)}{|\cos\bar{\theta}_i\cdot v-\sin\bar{\theta}_i\cdot u|},\ \frac{(\Delta x/\Delta s_i)}{|\cos\bar{\theta}_i\cdot v-\sin\bar{\theta}_i\cdot u-c|},\right.$$

$$\left.\frac{(\Delta x/\Delta s_i)}{|\cos\bar{\theta}_i\cdot v-\sin\bar{\theta}_i\cdot u+c|}\right\}=\mathrm{Min}\left\{\frac{(\Delta x/\Delta s_i)}{|\cos\bar{\theta}_i\cdot v-\sin\bar{\theta}_i\cdot u|+c}\right\},\qquad(44)$$

$L_{HX}(\Delta t)$: M-scheme in regions $u\leqslant c$

$$\frac{\Delta t}{\Delta x}\leqslant \mathrm{Min}\left\{\frac{1}{u},\ \frac{1}{|u-c|},\ \frac{1}{u+c}\right\}_{sub}\doteqdot\frac{1}{2c_*},\qquad(45)$$

U-scheme in regions $u>c$

$$\frac{\Delta t}{\Delta x}\leqslant \mathrm{Min}\left\{\frac{2}{u},\ \frac{2}{u-c},\ \frac{2}{u+c}\right\}_{sup}=\mathrm{Min}\left\{\frac{2}{u+c}\right\}_{sup},\qquad(46)$$

where c_* is the critical sonic velocity, then,

$$\Delta t\leqslant \mathrm{Min}\left\{\frac{2\Delta y\cdot(\Delta x/\Delta s_i)}{|\cos\bar{\theta}_i\cdot v-\sin\bar{\theta}_i\cdot u|+c},\ \frac{\Delta x}{2c_*},\ \frac{2\Delta x}{(u+c)_{sup}}\right\}.\qquad(47)$$

In general, the Mach number of transonic flow is not high, and accordingly the first and third terms are greater than the second on the right-hand side of the condition (47) if $\Delta y=\Delta x$; thus, we have

$$\Delta t\leqslant\frac{\Delta x}{2c_*}.\qquad(48)$$

For the purpose of comparison, we calculated the same problem using the M-scheme throughout the flow field. Then the stability condition is changed to

$$\Delta t\leqslant \mathrm{Min}\left\{\frac{\Delta x}{(u+c)_{sup}}\right\}.\qquad(49)$$

Since the eigenvalue $u-c$ becomes equal to zero in the vicinity of sonic points, the fourth-order dissipative term is necessary for $L_{HX}(\Delta t)$. The ω value is determined by the condition (14) in regions $u\leqslant c$,

$$0\leqslant\omega<\mathrm{Min}\left\{1-\left[u\frac{\Delta t}{\Delta x}\right]^2,\ 1-\left[(u-c)\frac{\Delta t}{\Delta x}\right]^2,\ 1-\left[(u+c)\frac{\Delta t}{\Delta x}\right]^2\right\}$$

$$=1-\left[(u+c)\frac{\Delta t}{\Delta x}\right]^2.\qquad(50)$$

The boundary conditions in the upstream and upper farfield are freestream

ones. The values of ρ, ρu and ρv in the downstream boundary are found by the vanishing second-order differentials while e is determined from Eq. (37) by assigning $p=p_\infty$. The symmetry conditions are used along the axis of symmetry.

To calculate airfoil surface points, Eqs. (38) and (39) are replaced by one-side scheme; it is similar to the upwind scheme replacing ∇ by Δ and ∇^2 by $-\Delta^2$ in Eqs. (2) and (15), although it does not essentially mean "upwind". Thus, $L_{OY}(\Delta t)$ on airfoil surface is explicitly given by

$$\overline{U^{n+1/2}_{i,j}} = U^n_{i,j} - \frac{\Delta t}{\Delta y}\Delta H^n_{i,j}, \tag{51}$$

$$U^{n+1/2}_{i,j} = \frac{1}{2}(U^n_{i,j} + \overline{U^{n+1/2}_{i,j}}) - \frac{\Delta t}{2\Delta y}\Delta \overline{H^{n+1/2}_{i,j}} + \frac{\Delta t}{2\Delta y}\Delta^2 H^n_{i,j}, \tag{52}$$

which is second-order accurate in both time and space as well. $L_{HX}(\Delta t)$ on airfoil surface is identical to Eqs. (41), (42) and (43). After $U^{n+1}_{i,1}$ were obtained from Eq. (27), we modified the direction of velocity to be tangent to surface as follows:

$$\tilde{u}^{n+1}_{i,1} = \sqrt{(u^{n+1}_{i,1})^2 + (v^{n+1}_{i,1})^2} \cdot \cos\bar{\theta}_i, \tag{53}$$

$$\tilde{v}^{n+1}_{i,1} = \sqrt{(u^{n+1}_{i,1})^2 + (v^{n+1}_{i,1})^2} \cdot \sin\bar{\theta}_i. \tag{54}$$

The initial flow field as a starting condition is given artificially. The flow variables at the three special points are assumed as follows: The leading edge and trailing edge are stagnation points of freestream, while the highest point of airfoil surface has a dimensionless velocity value equal to $1+\delta/L$ which is heuristically assigned from the fact that the relative velocity of the highest point of a circle ($\delta/L=1$) is 2 in imcompressible potential flows. Besides, the downstream is assumed freestream as well, whereas the pressure is distributed linearly along symmetric axis and parabolically over the airfoil surface, and the flow variables are distributed linearly in Y-direction.

5. Calculated Results

We calculated three typical cases using 60×40 meshes with 20 gridpoints on the airfoil surface. The accuracy was maintained to the extent that the relative error for every flow variable could not exceed 0.001. Each of these cases converged in the vicinity of 550 time steps. It required about 120~150 seconds CPU time on FACOM M-382.

Fig. 3 shows the pressure distribution for the freestream Mach number 0.83. They were calculated using either the H-scheme or the M-scheme throughout the flow field. As shown in Fig. 3, the both results using the H-scheme and the M-scheme agreed with each other very well in most of the region ahead of shock. For the M-scheme, however, a spurious pressure oscillation appeared in the upstream points adjacent to shock. It did not appear for the H-scheme, which is one of the advantages of the H-scheme.

Fig. 4 compares the results of this analysis with the ones in Reference 1 for a freestream Mach number 0.83. As indicated in Fig. 4, the main difference is that the location of shock wave in this analysis is slightly behind the one in

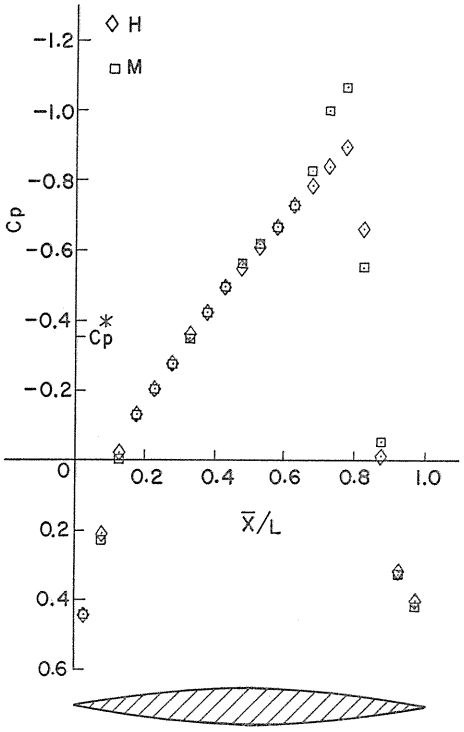

Fig. 3. Pressure distribution on a circular airfoil when M_∞=0.83 and thickness-to-chord ratio=0.10.

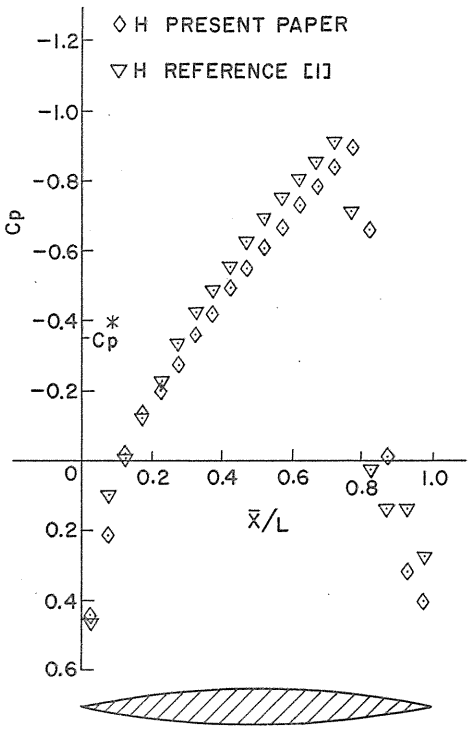

Fig. 4. The present pressure distribution compared with Reference 1.

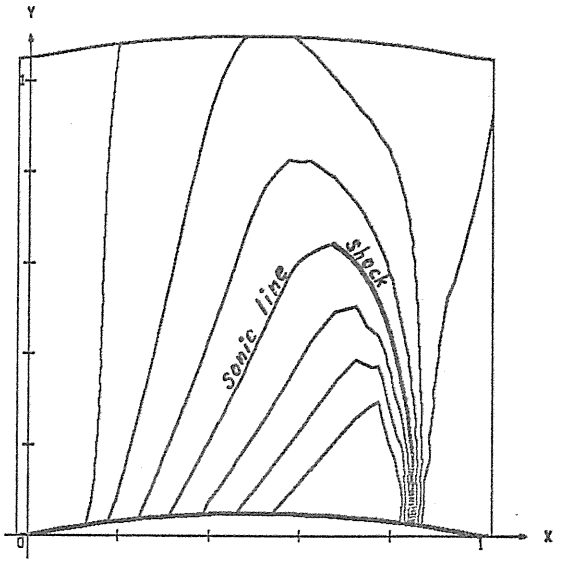

Fig. 5. The equi-Mach-number lines for M_∞=0.83.

Reference 1.

Fig. 5 shows the equi-Mach-number lines in the flow field calculated by the H-scheme for $M_\infty=0.83$.

We also calculated the case which utilized the H-scheme but did not take account of the geometric thickness of airfoil (all meshes are rectangular). The results show that the effect of thickness is negligibly small, as shown in the following table:

x	0.025	0.225	0.425	0.625	0.775	0.875	0.975
C_p $(\delta=0)$	0.419	−0.215	−0.503	−0.734	−0.900	0.002	0.396
C_p $(\delta\neq 0)$	0.438	−0.207	−0.498	−0.734	−0.899	−0.011	0.397

References

1) R. F. Warming and R. M. Beam: Upwind Second-Order Difference Schemes and Applications in Aerodynamic Flows, AIAA Journal, Vol. 14, September 1976, pp. 1241–1249.
2) C. M. Hung and R. W. MacCormack: Numerical Solutions of Supersonic and Hypersonic Laminar Compression Corner Flows, AIAA Journal, Vol. 14, April 1976, pp. 475–481.